



# <sup>1</sup>H NMR-based metabolomic profiling for identification of metabolites in *Capsicum annuum* cv. mirasol infected by beet mild curly top virus (BMCTV)



Nemesio Villa-Ruano<sup>a</sup>, Rodolfo Velásquez-Valle<sup>b</sup>, L. Gerardo Zepeda-Vallejo<sup>c</sup>,  
Nury Pérez-Hernández<sup>d</sup>, Manuel Velázquez-Ponce<sup>e</sup>, Victor M. Arcos-Adame<sup>f</sup>,  
Elvia Becerra-Martínez<sup>f,\*</sup>

<sup>a</sup> Universidad de la Sierra Sur, Guillermo Rojas Mijangos S/N, Miahuatlán de Porfirio Díaz CP 70800, Oaxaca, Mexico

<sup>b</sup> INIFAP-Campo Experimental Zacatecas, Km. 24.5 Carretera Zacatecas-Fresnillo. Apdo, Postal # 18. Calera de V. R. CP 98500, Zacatecas, Mexico

<sup>c</sup> Departamento de Química Orgánica, Escuela Nacional de Ciencias Biológicas, Instituto Politécnico Nacional, Ciudad de México 11340, Mexico

<sup>d</sup> Escuela Nacional de Medicina y Homeopatía, Instituto Politécnico Nacional, Ciudad de México 07320, Mexico

<sup>e</sup> Unidad Profesional Interdisciplinaria de Ingeniería Campus Guanajuato, Instituto Politécnico Nacional, Guanajuato 36275, Mexico

<sup>f</sup> Centro de Nanociencias y Micro y Nanotecnologías, Instituto Politécnico Nacional, Ciudad de México 07738, Mexico

## ARTICLE INFO

### Keywords:

*Capsicum annuum*

Beet mild curly top virus

Metabolomic profiling

<sup>1</sup>H NMR

Principal component analysis

## ABSTRACT

Beet mild curly top virus (BMCTV) is associated with an outbreak of curly top in chili pepper, tomato and other Solanaceae species, which can cause severe crop losses. The aim of this work was to obtain the <sup>1</sup>H NMR metabolomic profiling of both healthy chili peppers (cv. mirasol) and infected chili peppers with BMCTV in order to find chemical markers associated to the infection process. Significant differences were found between the two groups, according to principal component analysis and orthogonal projections to latent structure discriminant analysis. Compared to the asymptomatic peppers, the symptomatic fruits had higher relative abundance of fructose, isoleucine, histidine, phenylalanine and tryptophan. Contrarily, the asymptomatic samples showed greater amounts of malonate and isobutyrate. These results suggest that in diseased chili peppers there are metabolic changes related to the viral acquisition of energy for replication and capsid assembly. This is the first study describing the chemical profiling of a polar extract obtained from *Capsicum annuum* infected by BMCTV under open field conditions.

## 1. Introduction

Chili pepper (*Capsicum annuum* L.) is regarded as an essential condiment for many dishes around the world. It has been traditionally cultivated and consumed in Mexico for centuries, and today is still an integral part of Mexican food (Perry & Flannery, 2007). One of the most important economic activities in Mexico is the production and exportation of chili peppers (Velásquez-Valle et al., 2003). Besides its pungency used to add flavor to dishes, chili pepper is a source of various small molecules with nutraceutical activity, such as ascorbic acid, carotenoids, tocopherols, flavonoids and capsinoids (Conforti, Statti, & Menichini, 2007; Wahyuni et al., 2013).

The chili pepper plant is mostly cultivated in open fields where phytopathogens constantly pose a threat to crops. For instance, one of the main problems affecting the cultivation of chili peppers in north-central Mexico is the infection caused by begomovirus and curtovirus (Reveles-Torres et al., 2012). The yellowing of chili pepper is a common

disease derived from beet mild curly top virus (BMCTV) infection. Symptoms of this disease were described for the first time in 2003 and the pathogenic strain was finally characterized in 2008 (Velásquez-Valle, Medina-Aguilar, & Creamer, 2008). Plants infected with BMCTV show severe yellowing, upwardly rolled and small leaves, deformed fruits, dwarfism, chlorotic or yellow foliage on the whole plant, total or partial absence of reproductive structures (buds, flowers or fruits), elongated/thick leaves, and small and misshapen fruit (Reveles-Torres et al., 2012; Velásquez-Valle, Medina-Aguilar, & Creamer, 2008; Velásquez-Valle, Mena-Covarrubias, et al., 2012). As other chili diseases, BMCTV poses a risk to crop production that can result in severe monetary losses.

Pathogen recognition by host cells is generally linked to a morphological and physiological response, the latter of which usually includes an increase in energy consumption and changes in the metabolic pathways (Bolton, 2009; Berger, Sinha, & Roitsch, 2007). Currently, there is no available information about the effect of BMCTV on the

\* Corresponding author.

E-mail address: [elmartinez@ipn.mx](mailto:elmartinez@ipn.mx) (E. Becerra-Martínez).

metabolism of chili peppers. Insights in this respect may help to clarify the viral mechanisms during infection and thus potentially lead to alternatives for biological control.

For the metabolomic approach to the study of pathogen infections, the main analytical techniques are based on nuclear magnetic resonance (NMR) and mass spectrometry (MS) (Gomez-Casati, Zanor, & Busi 2013; Zhang et al., 2012). Unlike other techniques, NMR offers great selectivity and accuracy. When combined with multivariate statistical analysis, it is a powerful tool for comparing the chemical profiling of healthy and symptomatic plants (López-Gresa et al., 2012; Mahmud et al., 2015; Dos Santos Freitas et al., 2015). Therefore, the present study focused on the  $^1\text{H}$  NMR metabolomic profiling of chili peppers from *Capsicum annuum* cv. mirasol, comparing fruits with symptoms of BMCTV to healthy samples.

## 2. Materials and methods

### 2.1. Plant source

Symptomatic and asymptomatic samples of *Capsicum annuum* cv. mirasol were kindly provided by Dr. Rodolfo Velázquez-Valle from the INIFAP in Zacatecas, Mexico. On the symptomatic samples, he previously confirmed the presence of the virus with PCR tests (Velázquez-Valle, Medina-Aguilar, & Creamer, 2008; Velázquez-Valle, Reveles-Torres, Amador-Ramírez, Medina-Aguilar, & Medina-García, 2012). The chili pepper samples were harvested in the experimental field of that institution (Longitude: 102° 39' 34.0", Latitude: 22° 54' 31.3", Altitude: 2197 masl) during July–October in 2016. The current study was carried out with 25 diseased fruits and 25 healthy fruits. Diseased fruits were collected based on characteristic symptoms, whereas healthy fruits were chosen considering a similar color, size, texture and weight (Fig. 1). Similarity in color and texture among samples was estimated by harvester perception. Length, width and weight of the chili peppers were determined in accordance to the Mexican Official Norms (NMX-FF-025-SCFI-2014, Normas Oficiales Mexicanas, 2015). Measurement of the length was made from the base (excluding the peduncle) to the apex, and of the width at the widest point. The weight was read on an analytical balance (Table S1). Chili peppers were collected at the same hour every day and immediately frozen to minimize variation in metabolites caused by the circadian rhythm (Scognamiglio et al., 2015).

### 2.2. Chemicals

Deuterium oxide ( $\text{D}_2\text{O}$ , D 99.9 atom %) was purchased (Cambridge Isotope Laboratories, Inc.) and used as solvent. For  $^1\text{H}$  NMR analysis, 3-(trimethylsilyl)-1-propanesulfonic acid sodium salt (Sigma-Aldrich Co.; TSP, 97%) was the internal standard, while EDTA (ethylenediaminetetraacetic acid) and sodium azide ( $\text{NaN}_3$ ) (Merck™) were also added to the samples. NaOH and HCl (Sigma-Aldrich Co.) were employed to adjust pH.

### 2.3. Sample preparation

Each pepper was squeezed in a mortar and the juice was centrifuged for 20 min at 15,900g. For subsequent  $^1\text{H}$  NMR analysis, 900  $\mu\text{L}$  of the aqueous upper phase was mixed with 100  $\mu\text{L}$  of a solution containing 7 mM TSP, 10 mM EDTA, and 2 mM  $\text{NaN}_3$  in  $\text{D}_2\text{O}$ , at  $\text{pH } 5.42 \pm 0.05$ . Finally, 600  $\mu\text{L}$  of this solution were placed into 5 mm NMR tubes (Becerra-Martínez et al., 2017; Hohmann et al., 2014).

### 2.4. Nuclear magnetic resonance (NMR) experiments

NMR analysis was conducted on a Bruker 750 MHz spectrometer (Bruker Biospin, Rheinstetten, Germany) equipped with a 5 mm TXI cryoprobe. All the aqueous extracts from the mirasol peppers were measured at  $298.1 \pm 0.1$  K, without rotation and with 4 dummy scans prior to 64 scans. Acquisition parameters were set as follows: FID size = 64 K, spectral width = 19.9967 ppm, receiver gain = 1, acquisition time = 2.18 s, relaxation delay = 10 s, and FID resolution = 0.45 Hz. Data acquisition was achieved by NOESY pre-saturation pulse sequence (Bruker 1D noesypr1d) with water suppression via irradiation of the water frequency during the recycle and mixing time delays (Becerra-Martínez et al., 2017; Hohmann et al., 2014).

Several NMR experiments were performed with the aim of corroborating signal assignments. These analyses were based on  $^{13}\text{C}$  spectroscopy (Fig. S1), homonuclear correlation spectroscopy (2D  $^1\text{H}$ - $^1\text{H}$  COSY, Fig. S2), heteronuclear single quantum correlations (2D  $^1\text{H}$ - $^{13}\text{C}$  HSQC, Fig. S3, S4, S5, S6) and heteronuclear multiple bond correlation (2D  $^1\text{H}$ - $^{13}\text{C}$  HMBC, Fig. S7). The 2D NMR analysis was carried out on a Bruker 750 MHz spectrometer operating at 750.12 MHz ( $^1\text{H}$  frequency) and at 298 K. The parameters for the one-dimensional  $^1\text{H}$  NMR spectrum were: number of scans = 64, acquisition time = 2.18 s, relaxation delay = 1 s, spectral width = 15,000.0 Hz, and FID size = 65k data. For

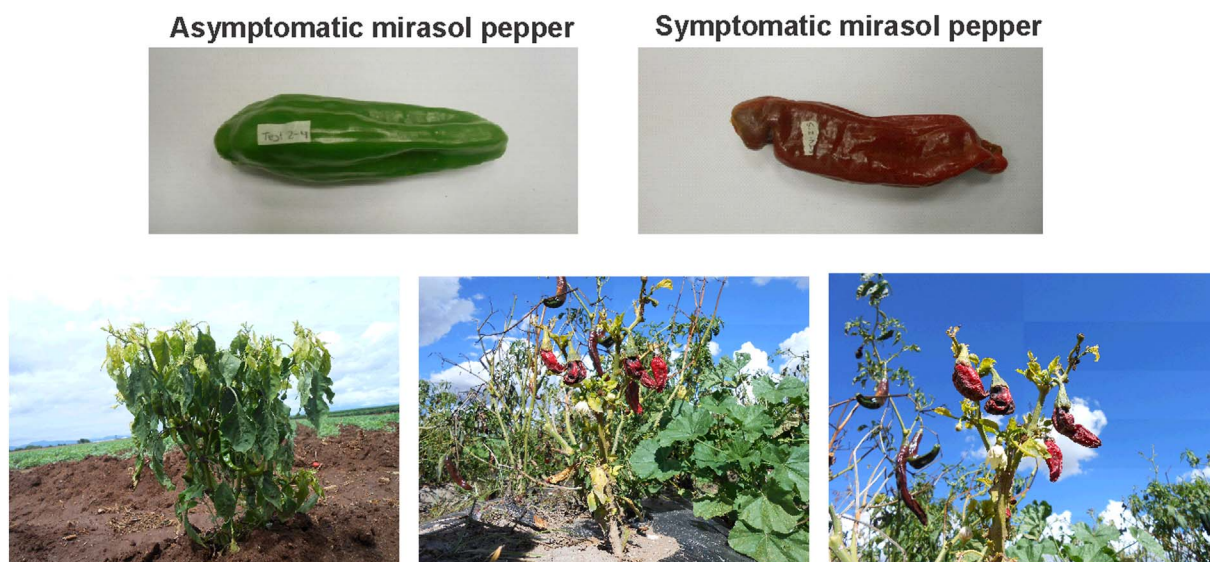


Fig. 1. Images of *Capsicum annuum* cv. mirasol grown in open fields, with symptoms of BMCTV infection.

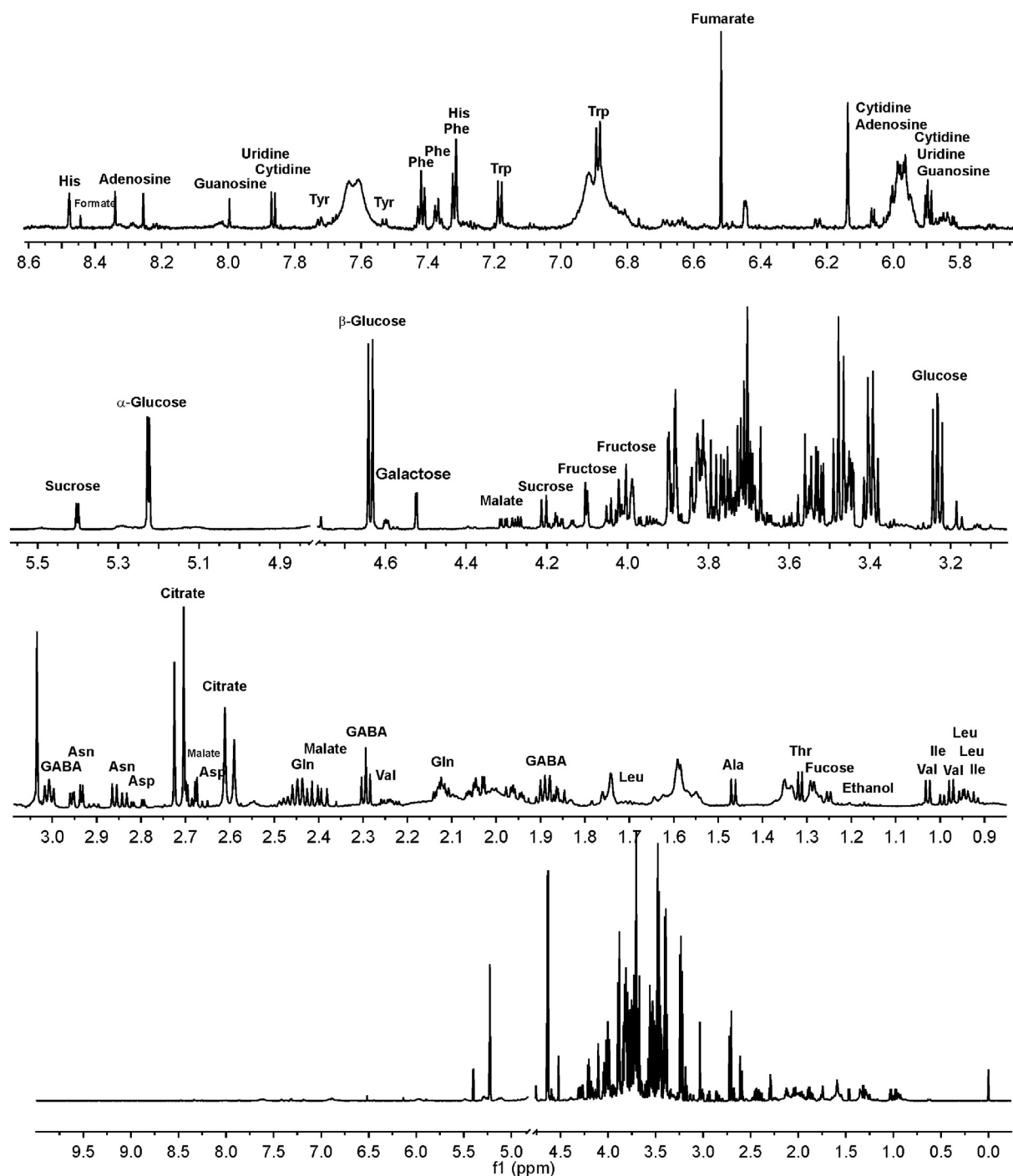


Fig. 2. Characteristic  $^1\text{H}$  NMR spectrum obtained at 750 MHz from aqueous extracts of *Capsicum annum* cv. mirasol. Signal assignments were based on 2D NMR experiments and the literature (Becerra-Martínez et al., 2017; Ritota et al., 2010).

the  $^{13}\text{C}$  NMR spectrum, the number of scans = 50,000.0, acquisition time = 0.71, relaxation delay = 2 s, spectral width = 45,454.5 Hz, and FID size = 64k data. COSY measurements were made with a spectral width of 7692.3 Hz in either dimension;  $2\text{k} \times 128$  were acquired with 128 scans per increment and a 2 s relaxation delay. For gHSQC, there were 1024 scans and 128 increments, with an acquisition time of 0.63 s and a relaxation delay of 1.5 s. The spectral width was 8012.8 and 38,806.4 Hz for the  $^1\text{H}$  and  $^{13}\text{C}$  dimensions, respectively, with  $^1J_{\text{CH}} = 145$  Hz. For gHMBC, there were 128 scans and 256 time increments, with an acquisition time of 0.65 s and a relaxation delay of 2 s. The spectral widths employed were the same as for gHSQC, with  $^1J_{\text{CH}} = 145$  Hz.

## 2.5. Metabolite profiling

Metabolites were identified by consulting the literature (Becerra-Martínez et al., 2017; Ritota et al., 2010) and corroborated by performing the aforementioned 1D and 2D NMR experiments (Table S2). Firstly, the  $^1\text{H}$  NMR spectra were automatically phased, and the baseline was corrected and calibrated to the TSP signal at 0.0 ppm with the MestReNova program (version 6.0.2; MestReC, Santiago de Compostela, Spain). The resulting  $^1\text{H}$  NMR spectra processed in MestReC were also imported into the Processor module of Chenomx NMR Suite version 8.2 (Chenomx, Edmonton, Canada), where they were subject to baseline correction, line broadening, phase correction and shim

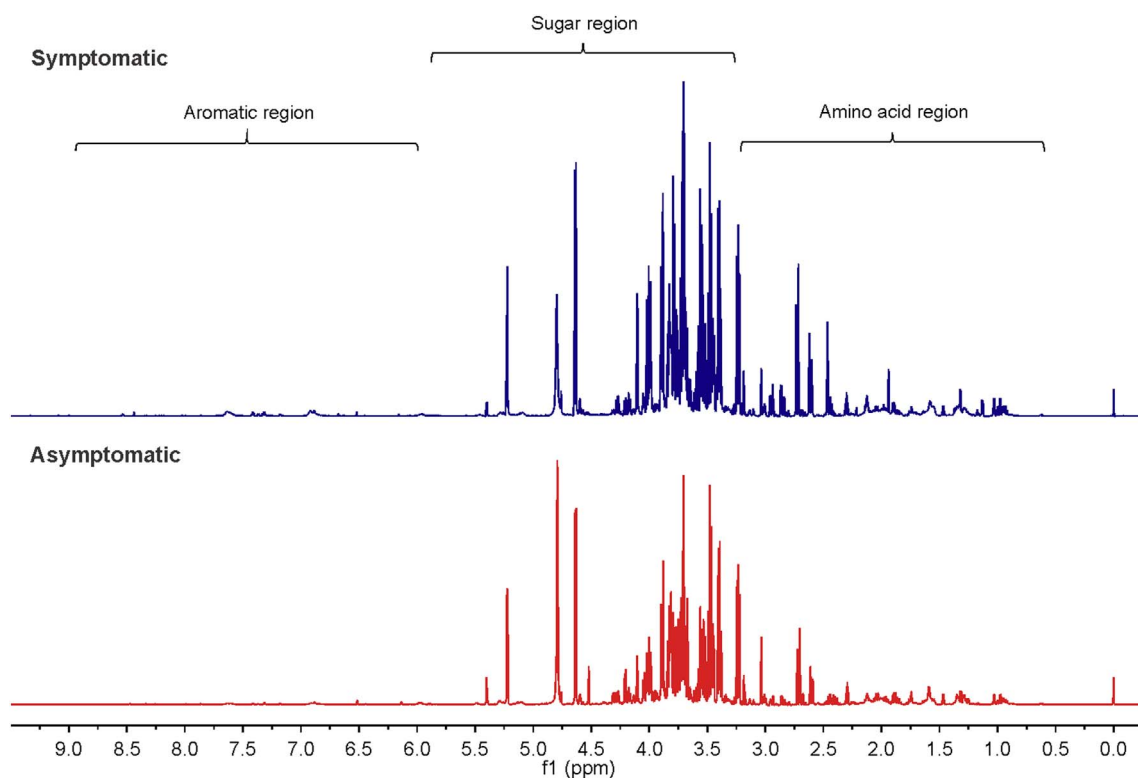


Fig. 3.  $^1\text{H}$  NMR spectra of aqueous extracts from asymptomatic (below) and symptomatic (above) fruits. The spectra, obtained at 750 MHz, were scaled in accordance with TSP (0.7 mM) as an internal standard.

correction. In this module, the spectra were calibrated to the signal of internal standard (TSP) and the pH was entered within a certain range (pH 4–9). The relative metabolite abundance was determined in the Profiler module. A list of compounds and their relative abundance was produced from each spectrum of a given sample, and then subjected to statistical analysis (Eun-Jeong et al., 2009; Duynhoven et al., 2013).

### 2.6. Multivariate statistical analysis

Chemometric analysis was performed with SIMCA version 13.0.3 (Umetrics, Kinnelon, NJ, USA) in the form of an unsupervised principal component analysis (PCA). A widely used multivariate analysis method in metabolomic studies and chemometrics in general, PCA has the purpose of reducing the number of predictive variables and solving the multi-collinearity problem (Maitra & Yan, 2008). With PCA, class differences were established from a multivariate dataset. To maximize the separation of class, orthogonal projections were made to latent structure discriminant analysis (OPLS-DA) (Worley & Powers, 2013). The quality of the model was described by  $R_x^2$  and  $Q^2$  values.  $R_x^2$  was defined as the proportion of the variance in the data observed in the model, and this parameter indicated goodness of fit.  $Q^2$  was defined as the proportion of variance in the data that was predictable by the model, and it denoted predictability (Wei et al., 2016; Jung et al., 2010).

### 2.7. Metabolic pathway analyses

To detect the possible differences in the biosynthesis of the metabolites between symptomatic and asymptomatic samples, pathway analysis was carried out with MetaboAnalyst 3.0 (<http://www.metaboanalyst.ca/MetaboAnalyst/>) (Eloh et al., 2016). MetaboAnalyst 3.0 was normalized by summation, log transformation and Pareto scaling (Jun-cai et al., 2017). Statistically significant differences were considered at  $p < 0.05$ .

## 3. Results and discussion

For the one-dimensional  $^1\text{H}$  NMR performed on healthy fruits of *Capsicum annum* cv. mirasol (Fig. 2), the 750 MHz spectra exhibited three main regions. The first one (0.5–3.0 ppm) contained signals of free amino acids such as alanine, asparagine, glutamine, isoleucine, leucine, valine and threonine, and organic acids including citric, malic and succinic acids. The second region (3.0–5.5 ppm) comprised signals corresponding to sucrose,  $\alpha$ -glucose,  $\beta$ -glucose and fructose. A weak signal was visible at 4.5–5.5 ppm, indicating the presence of galactose (identified as a double signal at 4.53 ppm). In the third region (6.0–9.0 ppm) there were relatively weak signals, which were associated with aromatic groups from amino acids and phenolic compounds. A visual inspection of the  $^1\text{H}$  NMR spectra revealed clear differences between the two groups in the levels of citrate, fructose, glucose and sucrose, as well as in some amino acids such as histidine, tryptophan and phenylalanine (Fig. 3).

The PCA score plots demonstrated statistically significant differences in metabolite composition between the two groups. The PCA model (Fig. 4A) set of three components showed  $R_x^2$  and  $Q^2$  values of 0.683 and 0.316, respectively. Asymptomatic chili peppers samples were clustered together, whereas the symptomatic ones were scattered, indicating individual differences between samples infected with BMCTV. The OPLS-DA model (Fig. 4B), consisting of one predictive and two orthogonal components, gave  $R_x^2$ ,  $R_y^2$  and  $Q^2$  values of 0.828, 0.997 and 0.956, respectively. The random permutation test (200 times) on the OPLS-DA model confirmed the differences between asymptomatic and symptomatic mirasol peppers (Fig. 4C). The y-intercept for  $R^2$  was 0.357 and for  $Q^2$  –0.462, supporting the validation of the model because the intercept for  $R^2$  was  $< 0.4$  and for  $Q^2$   $< 0.05$  (Eriksson et al., 2013).

According to the current results,  $^1\text{H}$  NMR and 2D NMR techniques coupled to OPLS-DA models can be used for the simultaneous and accurate identification of organic compounds, including sugars, amino

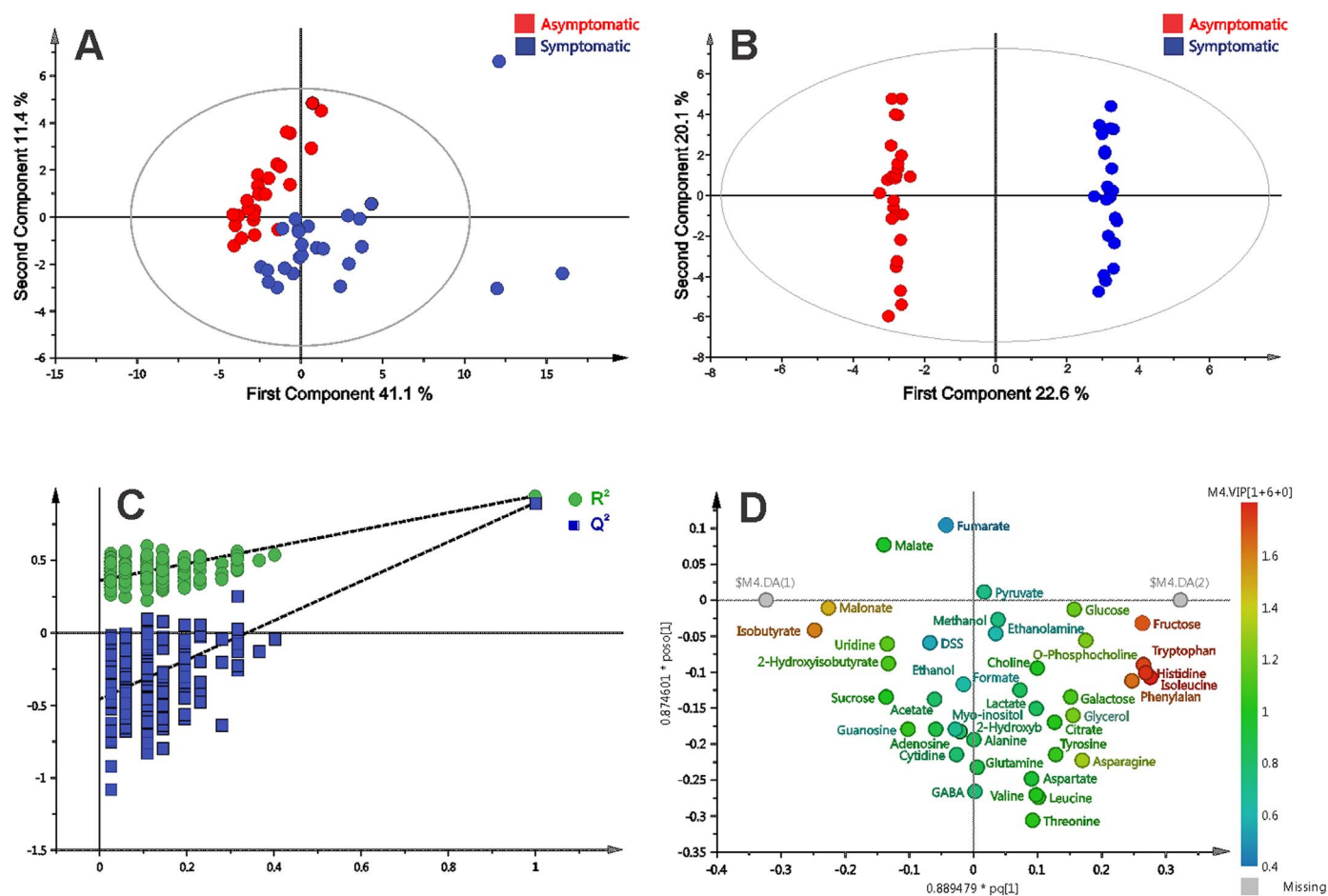


Fig. 4. PCA (A) and OPLS-DA (B) score plots generated from the  $^1\text{H}$  NMR spectra (750 MHz) of asymptomatic (red) and symptomatic (blue) samples. Statistical validation of the OPLS-DA model is shown, using permutation analysis for discrimination (C). The corresponding loading of scatter plots derived from targeted profiling of mostly secondary metabolites is illustrated (D). (For interpretation of the references to color in this figure legend, the reader is referred to the web version of this article.)

acids, organic acids and other compounds, as previously reported (Becerra-Martínez et al., 2017; Ritota et al., 2010). The presence of these metabolites as well as their chemical shifts and relative abundance are listed in Tables 1 and S2.  $^1\text{H}$  NMR spectra obtained at 750 MHz revealed a clear difference in the signal intensity, mainly for the sugar region.

Virus infection usually affects the metabolism and transport of primary carbohydrates in host plants (Shalitin & Wolf, 2000). Chili peppers showing symptoms of BMCTV infection displayed an increase in the levels of fructose and glucose (Table 1), which coincided with previous studies on the acute infection periods of potato virus Y and cucumber mosaic virus in their respective host (Shalitin & Wolf, 2000; Sindelarova, Sindelar, & Burketova, 1999). The concentration of sucrose was quite different between asymptomatic and symptomatic samples, suggesting the triggering of invertase during the BMCTV infection. Further research is required to determine the specific invertase genes involved in the susceptibility to BMCTV infection, and their mechanism of expression.

Interestingly, there are scarce reports on invertase expression mediated by proteinaceous inhibitors during a viral infection. The effect of their overexpression and/or repression could be considered as a potential alternative for regulating viral replication (Tauzin & Giardina, 2014). Although glucose and fructose may be functioning as alternate biochemical signals, their abundance in symptomatic samples should be related to their role as energy sources (glycolysis/pentose phosphate pathway) for viral replication (Shalitin & Wolf, 2000; Sindelarova, Sindelar, & Burketova, 1999). In the same context, the slight increase in galactose in plants infected with BMCTV could possibly be required in

glycoprotein synthesis for capsid assembly (Fernández-Fernández et al., 2002). Remarkably, changes were perceived in myo-inositol, an osmoregulator. Some studies suggest that alterations in the levels of myo-inositol are associated with tissue deformation during acute viral infection (Srivastava et al., 2012).

Overall, amino acid content was higher in symptomatic than in asymptomatic samples (Table 1), which has been reported for diverse plant hosts infected with specific viral species, at the initial and/or middle stages of infection (Biswas, 2017). It has been proposed that glutamine, asparagine and 4-aminobutyrate (GABA), known to be biosynthetically interconnected, are involved in plant stress responses related to pathogen infections (López-Gresa et al., 2012). In the current contribution, the content of asparagine rose significantly in infected chili peppers, suggesting a quick conversion of glutamate (undetectable) into glutamine and finally into asparagine. On the other hand, glutamate decarboxylation into GABA might also occur to a lesser extent. The low GABA levels observed in asymptomatic and symptomatic samples could be produced by abiotic stress (Shelp et al., 2012), an effect similar to that described for the systemic response of tomatoes by tomato mosaic virus infection (López-Gresa et al., 2012).

Although other studies have reported an increase in the levels of alanine due to potato virus Y, cucumber mosaic virus, yellow leaf curl virus and tomato mosaic virus (under the conditions of the assays) (Shalitin & Wolf, 2000; Sindelarova, Sindelar, & Burketova, 1999; Biswas, 2017; López-Gresa et al., 2012; Moshe et al., 2012), BMCTV infection does not seem to generate this effect. According to PCA and OPLS-DA analysis (Fig. 4D), histidine, isoleucine, tryptophan and phenylalanine were found in relative abundance in symptomatic samples

**Table 1**

<sup>1</sup>H NMR signals used to obtain integral regions for metabolites identified in *Capsicum annuum* cv. mirasol, along with the variation in the average relative abundance and coefficient of variation (CV) (expressed as a percentage) in the asymptomatic and symptomatic groups.

	Metabolite	Chemical shifts (ppm), <i>J</i> (Hz), multiplicity	Asymptomatic		Symptomatic	
			Variation	CV	Variation	CV
<b>Sugars</b>						
1	Fructose	4.01 (dd, <i>J</i> = 12.7, 1.3 Hz)	↓↓	30.60	↑↑	28.69
2	Galactose	54.73 (d, <i>J</i> = 1.9 Hz)	↓	31.70	↑	41.19
3	Glucose (α, β isomers)	3.23 (dd, <i>J</i> = 9.4, 8.0 Hz)	↓	36.22	↑	31.50
4	Myo-inositol	3.27 (t, <i>J</i> = 9.4 Hz)	=	25.11	=	33.67
5	Sucrose	4.21 (d, <i>J</i> = 8.8 Hz)	↑↑	26.63	↓↓	33.16
<b>Amino acids</b>						
6	Alanine	1.46 (d, 7.2)	=	34.25	=	30.91
7	Asparagine	2.85 (dd, <i>J</i> = 16.9, 7.8 Hz), 2.95 (dd, <i>J</i> = 16.9, 4.2 Hz)	↓↓	30.26	↑↑	37.71
8	Aspartate	2.67 (dd, <i>J</i> = 18.9, 7.4 Hz), 2.81 (dd, <i>J</i> = 17.5, 3.7 Hz)	=	41.90	=	33.74
9	4-Aminobutyrate	2.29 (t, <i>J</i> = 7.6 Hz)	=	30.94	=	31.05
10	Glutamine	2.11 (m), 2.14 (m)	↓	31.97	↑	31.18
11	Histidine	8.49 (m)	↓↓	33.91	↑↑	31.19
12	Isoleucine	0.93 (t, <i>J</i> = 7.4 Hz), 1.00 (d, <i>J</i> = 7.0 Hz)	↓↓	30.81	↑↑	24.50
13	Leucine	0.94 (d, <i>J</i> = 6.2 Hz), 0.95 (d, <i>J</i> = 6.2 Hz)	=	44.21	=	35.91
14	Phenylalanine	7.32 (d, <i>J</i> = 7.5), 7.37 (m), 7.42 (t, <i>J</i> = 7.5 Hz)	↓↓	46.24	↑↑	34.92
15	Threonine	1.32 (d, <i>J</i> = 6.6 Hz)	↓	41.04	↑	36.82
16	Tryptophan	7.53 (d, <i>J</i> = 8.3 Hz), 7.72 (d, <i>J</i> = 8.2 Hz)	↓↓	28.50	↑↑	30.06
17	Tyrosine	7.18 (d, <i>J</i> = 7.18 Hz)	↓	40.11	↑	32.39
18	Valine	0.98 (d, <i>J</i> = 7.0 Hz), 1.03 (d, <i>J</i> = 7.0 Hz)	↓	30.99	↑	34.15
<b>Organic acids</b>						
19	Acetate	1.92 (s)	=	46.17	=	35.13
20	Citrate	2.65 (d, <i>J</i> = 15.6 Hz), 2.75 (d, <i>J</i> = 15.6 Hz)	↓↓	32.56	↑	39.83
21	Formate	8.44 (s)	↓↓	35.38	↑↑	31.85
22	Fumarate	6.52 (s)	↑	24.46	↓	37.13
23	Lactate	1.31 (d, <i>J</i> = 6.6 Hz)	↓	31.09	↑	31.80
24	Malate	2.41 (dd, <i>J</i> = 15.5, 9.9 Hz), 2.69 (dd, <i>J</i> = 15.5, 3.2 Hz)	↑	33.05	↓	31.75
25	Malonate	3.10 (s)	↑↑	36.41	↓↓	38.67
26	Pyruvate	2.36 (s)	=	35.08	=	32.18
<b>Alcohols</b>						
27	Ethanol	1.17 (t, <i>J</i> = 7.1 Hz)	=	30.57	=	37.33
28	Ethanolamine	3.13 (t, <i>J</i> = 5.2 Hz)	=	28.93	=	30.02
29	Methanol	3.35 (s)	↓	25.25	↑	44.84
30	Glycerol	3.64 (dd, <i>J</i> = 17.2, 6.1 Hz)	↓	27.27	↑	37.26
<b>Nucleosides</b>						
31	Adenosine	8.25 (s)	=	24.76	=	36.14
32	Cytidine	7.85 (d, <i>J</i> = 7.2 Hz)	=	37.43	=	24.45
33	Guanosine	7.99 (s)	=	44.86	=	42.15
34	Uridine	7.86 (d, <i>J</i> = 8.1 Hz)	↑	35.83	↓	51.49
<b>Other compounds</b>						
35	2-Hydroxybutyrate	0.93 (t, <i>J</i> = 7.6 Hz)	=	40.36	=	28.69
36	2-Hydroxyisobutyrate	1.33 (s)	↑	41.07	↓	–
37	Choline	3.19 (s)	↓	35.90	↑	28.75
38	Isobutyrate	1.08 (d, <i>J</i> = 7.0 Hz)	↑↑	38.66	↓↓	–
39	Phosphocholine	3.21 (s)	↓	29.89	↑	38.53

s = singlet, d = doublet, t = triplet, m = multiplet, dd = doublet of doublets.

↑, increase; ↓, decrease; =, no change.

(Fig. 5), suggesting a link to amino acid recycling as a consequence of the transamination process (Biswas, 2017). These changes were simultaneous with a rise in the level of citric acid (Table 1), revealing evident modifications in the metabolism of keto acids. On the contrary, PCA and OPLS-DA analysis indicate that malonate and isobutyrate are differentially expressed in asymptomatic samples (Fig. 4D, 5), and *t*-tests evidenced statistically significant differences between the two groups ( $p \leq 0.05$ ). A previous study on the infection of tomato leaves by tomato yellow leaf curl virus showed a triggering of malonate and butyrate after 48 days post inoculation under greenhouse conditions (Moshe et al., 2012). Isobutyrate is a product of microbial activity that could stem from bacterial endophytes or opportunistic pathogens. Alternatively, malonate is apparently involved in the symbiotic nitrogen metabolism of plants (Kim, 2012). Since the chili peppers were herein collected in open fields, it cannot be discarded that there was an interaction of the fruits collected with natural microflora. Low levels of

these metabolites in asymptomatic samples are probably produced by the competitive action of BMCTV for host metabolism during acute infection.

In silico predictions of metabolic pathway alterations (using MetaboAnalyst 3.0) suggested that 13 pathways were affected, based on the statistically significant values ( $p < 0.05$ ) and an impact factor threshold  $> 0$  (Zhao et al., 2016). These predictions are consistent with the observed changes in relative abundance for each metabolite and with the results of the statistical models employed. According to the free software (Fig. 6), modifications were identified in the biosynthesis of essential (for humans) amino acids such as tryptophan, histidine, phenylalanine, valine and leucine, and consequently in the metabolism of glycine, serine, alanine, threonine, aspartate and glutamate (dicarboxylates). Additionally, the software predicted modifications in the production of glycerophospholipids and in glyoxylate metabolism (Fig. 6).

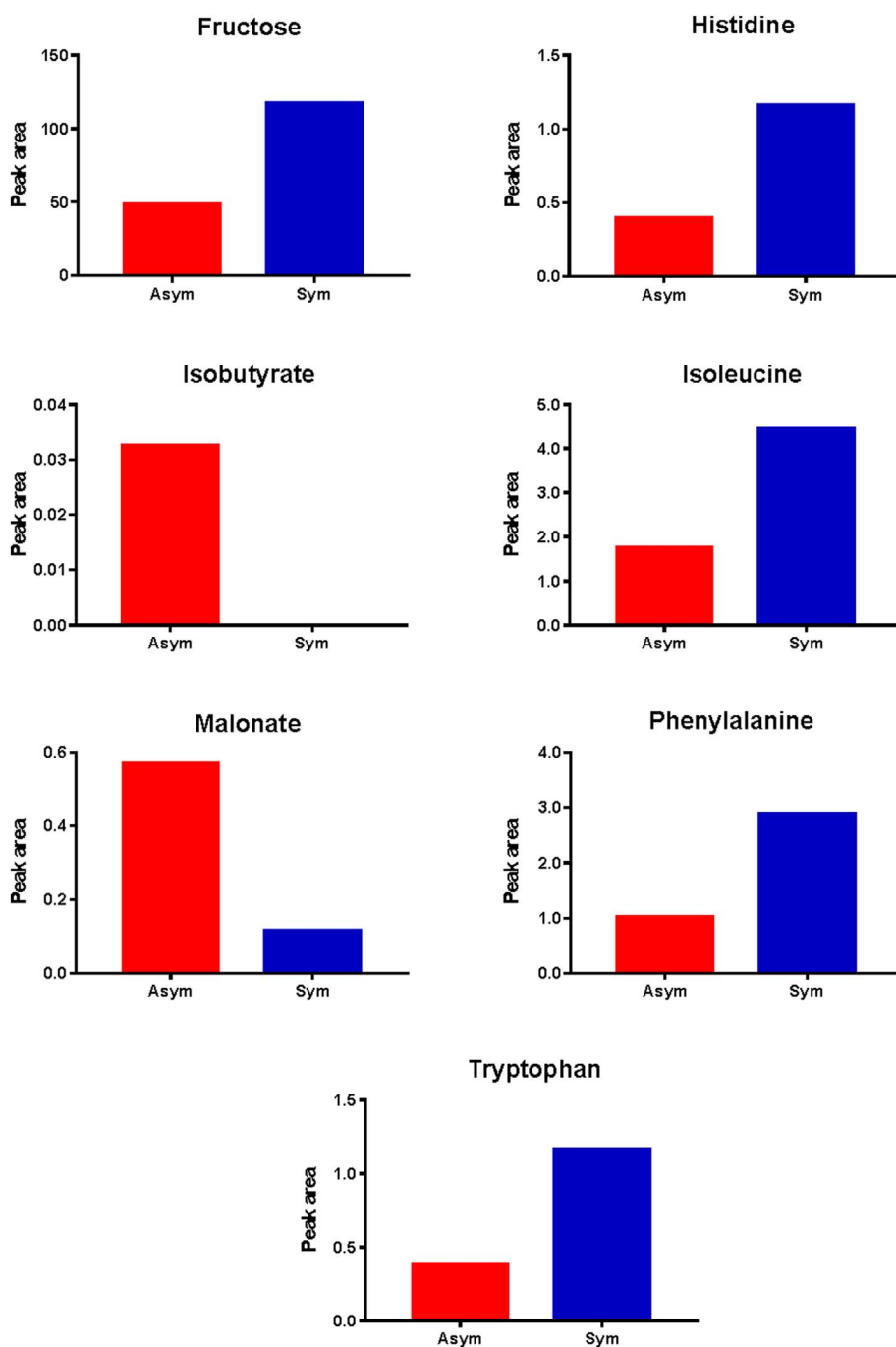


Fig. 5. Relative abundance of metabolites based on the mean peak area of the associated signals from 750 MHz  $^1\text{H}$  NMR spectra of symptomatic and asymptomatic mirasol pepper groups. Data are expressed as the mean  $\pm$  standard error, calculated using twenty replicates.

It can be assumed that the alterations in the metabolism of starch, sucrose and galactose cause side effects in the entire metabolic network, since these carbohydrates either play a key role as a source of energy for vital enzymatic reactions or have important structural functions (Fig. 6). Table S3 shows some pathways affected by BMCTV infection. Further research is required to determine differences in the metabolic profiling of the hydrophobic fraction from *Capsicum annuum* cv. mirasol in relation to plants cultivated under greenhouse conditions versus those grown in open fields with BMCTV infection.

#### 4. Conclusion

*Capsicum annuum* cv. mirasol chili peppers with symptoms of BMCTV infection exhibited an evident variation in the level and variety of metabolites when compared to asymptomatic fruits. There was

chemical variability between the two groups of samples in the carbohydrate and amino acid content. This strongly suggests that the acute infection of *Capsicum annuum* cv. mirasol by BMCTV caused alterations affecting viral acquisition of energy and the production of monomers for replication and capsid assembly. Due to metabolic changes in the carbohydrate reserve, and specifically in sucrose metabolism, the possible regulation of BMCTV replication by the overexpression of proteinaceous inhibitors of invertase activity should be explored. Additionally, the effect of BMCTV infection in RNA-silencing plants, particularly the modifications in certain invertase genes, should also be examined. Insights into these topics could possibly lead to novel alternatives for the biological control of BMCTV.

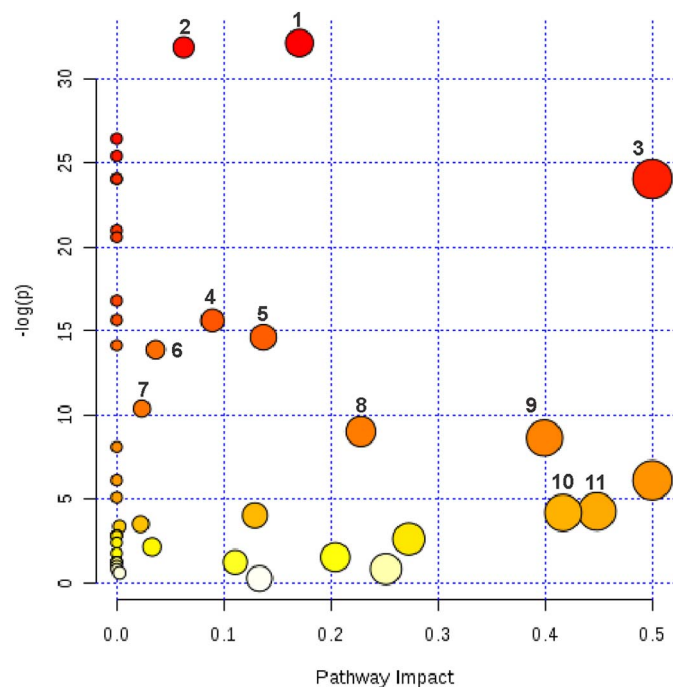


**Fig. 6.** Alterations in the metabolic pathways of *Capsicum annuum* cv. mirasol infected with BMCVT, detected by using MetaboAnalyst 3.0. Differences were considered statistically significant with  $p$  values  $< 0.05$  and an impact factor threshold  $> 0.1$ . 1) Tryptophan metabolism, 2) histidine metabolism, 3) phenylalanine metabolism, 4) starch and sucrose metabolism, 5) glycine, serine and threonine metabolism, 6) valine, leucine and isoleucine biosynthesis, 7) glycerophospholipid metabolism, 8) glyoxylate and dicarboxylate metabolism, 9) galactose metabolism, 10) alanine, aspartate and glutamate metabolism, and 11) methane metabolism.

## Acknowledgments

This research received financial support from SIP-IPN 20170405.

## Appendix A. Supplementary data

Supplementary data to this article can be found online at <https://doi.org/10.1016/j.foodres.2018.01.065>.

## References

- Becerra-Martínez, E., Florentino-Ramos, E., Pérez-Hernández, N., Zepeda-Vallejo, L. G., Villa-Ruano, N., Velásquez-Ponce, M., ... Bañuelos-Hernández, A. E. (2017).  $^1\text{H}$  NMR-based metabolomic fingerprinting to determine metabolite levels in serrano peppers (*Capsicum annuum* L.) grown in two different regions. *Food Research International*, 102, 163–170.
- Berger, S., Sinha, A. K., & Roitsch, T. (2007). Plant physiology meets phytopathology: Plant primary metabolism and plant-pathogen interactions. *Journal of Experimental Botany*, 58(15), 4019–4026.
- Biswas, K. K. (2017). *Plant viruses, diseases and their management* (1st ed.). Delhi, India: I. K. International Publishing House 28.
- Bolton, M. D. (2009). Primary metabolism and plant defense—fuel for the fire. *Molecular Plant Microbe Interaction*, 22(5), 487–497.
- Conforti, F., Statti, G. A., & Menichini, F. (2007). Chemical and biological variability of hot pepper fruits (*Capsicum annuum* var. *acuminatum* L.) in relation to maturity stage. *Food Chemistry*, 102(4), 1096–1104.
- Dos Santos Freitas, D., Fermino Carlos, E., Soares de Souza Gil, M. C., Gonzaga Esteves Vieira, L., & Braz Alcantara, G. (2015). NMR-based metabolomic analysis of huanglongbing-asymptomatic and -symptomatic citrus trees. *Journal Agricultural Food Chemistry*, 63(34), 7582–7588.
- Duynhoven, J. V., Van As, H., Belton, P. S., & Webb, G. A. (2013). *Magnetic resonance in food science: Food for thought* (1st ed.). I, Cambridge, United Kingdom: RSC Publishing 3–13.
- Eloh, K., Sasanelli, N., Maxia, A., & Caboni, P. (2016). Untargeted metabolomics of tomato plants after root-knot nematode infestation. *Journal Agricultural Food Chemistry*, 64(29), 5963–5968.
- Eriksson, K., Johansson, E., Trygg, J., & Vikstrom, C. (2013). *Multi and megavariable data analysis: Basis principles and application* (4th ed.). Sweden: Umetrics Academy (Chapter 1, 8).

- Eun-Jeong, L., Shaykhtudinov, R., Weljie, A. M., Vogel, H. J., & Facchini, P. J. (2009). Quality assessment of ginseng by  $^1\text{H}$  NMR metabolite fingerprinting and profiling analysis. *Journal Agricultural Food Chemistry*, 57(16), 7513–7522.
- Fernández-Fernández, M., Camafeita, E., Bonay, P., Méndez, E., Albar, J. P., & García, J. A. (2002). The capsid protein of a plant single-stranded RNA virus in modified by O-linked N-acetylglucosamine. *Journal of Biological Chemistry*, 277(1), 135–140.
- Gomez-Casati, D. F., Zanor, M. I., & Busi, M. V. (2013). Metabolomics in plants and humans: Applications in the prevention and diagnosis of diseases. *BioMed Research International*, 2013, 1–11.
- Hohmann, M., Christoph, N., Wachter, H., & Holzgrabe, U. (2014).  $^1\text{H}$  NMR profiling as an approach to differentiate conventionally and organically grown tomatoes. *Journal Agricultural Food Chemistry*, 62(33), 8530–8540.
- Jun-cai, D., Cai-qiong, Y., Jing, Z., Qing, Z., Feng, Y., Wen-yu, Y., & Jiang, L. (2017). Organ-specific differential NMR-based metabolomic analysis of soybean [*Glycine max* (L.) Merr.] fruit reveals the metabolic shifts and potential protection mechanisms involved in field mold infection. *Frontiers in Plant Science*, 8, 1–11.
- Jung, Y., Lee, J., Kwon, J., Kwang-Sik, L., Ryu, D. H., & Geum-Sook, H. (2010). Discrimination of the geographical origin of beef by  $^1\text{H}$  NMR-based metabolomics. *Journal Agricultural Food Chemistry*, 58(19), 10458–10466.
- Kim, Y. S. (2012). Malonate metabolism: Biochemistry, molecular biology, physiology, and industrial application. *Journal of Biochemistry and Molecular Biology*, 35(5), 443–451.
- López-Gresa, M. P., Lisón, P., Kim, H. K., Choi, Y. H., Verpoorte, R., Rodrigo, I., ... Bellés, J. M. (2012). Metabolic fingerprinting of tomato mosaic virus infected *Solanum lycopersicum*. *Journal of Plant Physiology*, 169(16), 1586–1596.
- Mahmud, I., Kousik, C., Hassell, R., Chowdhury, K., & Boroujerdi, A. F. (2015). NMR spectroscopy identifies metabolites translocated from powdery mildew resistant rootstocks to susceptible watermelon scions. *Journal Agricultural Food Chemistry*, 63(36), 8083–8091.
- Maitra, S., & Yan, J. (2008). Principle component analysis and partial least squares: Two-dimension reduction techniques for regression. *Casualty Actuarial Society*, 79–90.
- Moshe, A., Pfannstiel, J., Yariv, B., Kolot, M., Sobol, I., Czosnek, H., & Gorovits, R. (2012). Stress responses to tomato yellow leaf curl virus (TYLCV) infection of resistant and susceptible tomato plants are different. *Metabolomics*, 1, 2–13.
- Normas Oficiales Mexicanas (2015). Productos alimenticios no industrializados para consumo humano-chile fresco (*Capsicum* spp). *Tech. rep. NMX-FF-025-SCFI-2014*. México: Normas Oficiales Mexicanas.
- Perry, L., & Flannery, K. V. (2007). Precolumbian use of chili peppers in the valley of Oaxaca, Mexico. *Proceedings of the National Academy of Sciences*, 104(29), 11905–11909.
- Reveles-Torres, L. R., Velásquez-Valle, R., Mauricio-Castillo, J. A., & Salas-Muñoz, S. (2012). Detección de infecciones mixtas causadas por begomovirus y curtovirus en plantas de chile para secado en San Luis Potosí. *Revista Mexicana de Fitopatología*, 30(2), 155–160.
- Ritota, M., Marini, F., Sequi, P., & Valentini, M. (2010). Metabolomic characterization of Italian sweet pepper (*Capsicum annuum* L.) by means of HRMAS-NMR spectroscopy and multivariate analysis. *Journal Agricultural Food Chemistry*, 58(17), 9675–9684.
- Scognamiglio, M., D'Abrosca, B., Assunta Esposito, A., & Fiorentino, A. (2015). Chemical composition and seasonality of aromatic Mediterranean plant species by NMR-based metabolomics. *Journal of Analytical Methods in Chemistry*, 1–9.
- Shalitin, D., & Wolf, S. (2000). Cucumber mosaic virus infection affects sugar transport in melon plants. *Plant Physiology*, 123(2), 597–604.
- Shelp, B. J., Bozzo, G. G., Trobacher, C. P., Zarei, A., Deyman, K. L., & Briki, C. J. (2012). Hypothesis/review: Contribution of putrescine to 4-aminobutyrate (GABA) production in response to abiotic stress. *Plant Science*, 194, 130–135.
- Sindelarova, M., Sindelar, L., & Burketova, L. (1999). Changes in glucose, fructose and saccharose metabolism in tobacco plants infected with potato virus Y. *Biologia Plantarum*, 42(3), 431–439.
- Srivastava, S., Bisht, H., Sidhu, O. P., Srivastava, A., Singh, P. C., Pandey, R. M., ... Nautiyal, C. S. (2012). Changes in the metabolome and histopathology of *Amaranthus hypochondriacus* L. in response to Ageratum enation virus infection. *Phytochemistry*, 80, 8–16.
- Tauzin, A. S., & Giardina, T. (2014). Sucrose and invertases, a part of the plant defense response to the biotic stresses. *Frontiers Plants Science*, 5, 1–8.
- Velásquez-Valle, R., Medina-Aguilar, M. M., & Creamer, R. (2008). First report of *Beet mild curly top virus* infection of chili pepper in north-central Mexico. *Plant Disease*, 92(4), 650.
- Velásquez-Valle, R., Medina-Aguilar, M. M., & Macías-Valdez, L. M. (2003). Reacción de líneas avanzadas de chile (*Capsicum annuum* L.) provenientes de Zacatecas a enfermedades comunes en Aguascalientes, México. *Revista Mexicana de Fitopatología*, 21(1), 71–74.
- Velásquez-Valle, R., Mena-Covarrubias, J., Reveles-Torres, L. R., Argüello-Astorga, G. R., Salas-Luévano, M. A., & Mauricio-Castillo, J. A. (2012). First report of *Beet mild curly top virus* in dry bean in Zacatecas, Mexico. *Plant Disease*, 96(5), 771.
- Velásquez-Valle, R., Reveles-Torres, L. R., Amador-Ramírez, M. D., Medina-Aguilar, M. M., & Medina-García, G. (2012). Presencia de *Circulifer tenellus* Baker y *Beet mild curly top virus* en maleza durante el invierno en el centro norte de México. *Revista Mexicana de Ciencias Agrícolas*, 3(4), 813–819.
- Wahyuni, Y., Ballester, A. R., Tikunov, Y., Vos, R. C. H., Pelgrom, K. T. B., Maharjaya, A., ... Bovy, A. G. (2013). Metabolomics and molecular marker analysis to explore pepper (*Capsicum* sp.) biodiversity. *Metabolomics*, 9(1), 130–144.
- Wei, F., Furihata, K., Zhang, M., Miyakawa, T., & Tanokura, M. (2016). Use of NMR-based metabolomics to chemically characterize the roasting process of chicory root. *Journal of Agricultural and Food Chemistry*, 64(33), 6459–6465.
- Worley, B., & Powers, R. (2013). Multivariate analysis in metabolomics. *Current Metabolomics*, 1(1), 92–107.
- Zhang, A., Sun, H., Wang, P., Han, Y., & Wang, X. (2012). Modern analytical techniques in metabolomics analysis. *Analyst*, 137(2), 293–300.
- Zhao, L., Huang, Y., Zhou, H., Adeleye, A. S., Wang, H., Cruz Ortiz, C., ... Keller, A. A. (2016). GC-TOF-MS based metabolomics and ICP-MS based metalomics of cucumber (*Cucumis sativus*) fruits reveal alteration of metabolites profile and biological pathway disruption induced by nano copper. *Environmental Science Nano*, 3, 1114–1123.